Formation, Classification, and Properties of Soils at Two Relict Charcoal Hearth Sites in Brandenburg, Germany

Florian Hirsch [1]*, Anna Schneider [1], Albrecht Bauriegel [2], Alexandra Raab [1,3] and Thomas Raab [1]

[1] Geopedology and Landscape Development, Brandenburgische Technische Universität Cottbus-Senftenberg, Cottbus, Germany, [2] Landesamt für Bergbau, Geologie und Rohstoffe Brandenburg, Cottbus, Germany, [3] Chair of Environmental Economics, Brandenburgische Technische Universität Cottbus-Senftenberg, Cottbus, Germany

Historical charcoal production can have significant effects on soil properties. We studied soils at former charcoal production sites (relict charcoal hearths, RCHs) and compared these soils with undisturbed soil next to the charcoal hearths and four typical soils on similar parent material located at distances between 10 and 70 km from the RCHs. In a landscape typical of the northern German lowland, we found Podsolige Braunerde [WRB: Brunic Arenosols (Protospodic)] outside of the RCHs and soils with a clearly different stratigraphy within the RCHs. The main feature of the soils at both of the studied RCHs is a heterogeneous, charcoal-bearing deposit that is ∼30 cm thick. No indications of translocation or mineral transformation processes, which form distinct soil horizons after the deposition of anthropogenic material on the RCHs, are present. Except for the differences in color and total carbon content, the soil chemistry of the RCHs hardly differs from that of the soil outside of the charcoal hearth sites. The soil colors and magnetic susceptibility values strongly suggest that the RCH substrates and the underlying topsoil were affected by thermally induced transformation of iron (hydr-)oxides. Although the charring procedure normally requires ∼2 weeks, the heating effect only reaches to a maximum depth of 8 cm into the buried soil below the charcoal hearths. The presence of reddish soil and an abrupt increase in magnetic susceptibility in the upper 2 cm of the soil below the charcoal hearths indicate the heat-induced transformation of iron (hydr-)oxides into maghemite. Brighter soil color and an increase in soil organic matter (SOM) in the lower parts of the buried topsoil demonstrate the combustion of SOM up to 5 cm depth below the RCH. According to the German Guidelines for Soil Mapping, the soils in the RCHs are classified as Regosols above Braunerde [WRB: Spolic Technosols (Arenic)]. However, because the anthropogenic features of these soil sediments are disregarded in the German Guidelines for Soil Mapping, we suggest adapting the "M" horizon to permit a jM horizon. Thus, the soils in the RCHs could be classified as Kolluviale Braunerde.

Keywords: pyrolysis, soils, iron oxides, charcoal, micromorphology, soil classification

INTRODUCTION

Although the traditional production of charcoal in upright circular hearths ("*Platzmeiler*"; Groenewoudt, 2007) or modern brick-built kilns still plays an important role in the local economies of some parts of Africa and Asia (Chidumayo and Gumbo, 2013; Bolognesi et al., 2015), charcoal production for industrial processes is no longer economically relevant in industrial countries. From prehistoric times until the nineteenth century, the charring of wood in charcoal hearths was the base for metallurgic processes in Europe (Groenewoudt, 2007; Pèlachs et al., 2009). The demand for charcoal for metal production peaked from the thirteenth to nineteenth centuries in Europe (Pèlachs et al., 2009; Deforce et al., 2013; Knapp et al., 2015; Carrari et al., 2017; Criscuoli et al., 2017; Dupin et al., 2017; Krebs et al., 2017; Schmidt and Levy, 2017) and in the middle of the nineteenth century in North America (Mikan and Abrams, 1995; Straka, 2014; Raab T. et al., 2017). The production and use of wood charcoal ceased with the growing use of coal in North America and Europe in the mid-nineteenth century (Pasmore, 1964; Raab et al., 2015; Raab T. et al., 2017). Charcoal burning was a common handcraft and was often performed as a decentralized business in woodlands close to industrial sites with high energy demands, such as ironworks (Schneider et al., 2015; Raab A. et al., in press). Logs were gathered by felling trees in the immediate vicinity of future charcoal hearth sites, where colliers prepared platforms to stack the logs for charring. On hillslopes, the platforms were built on man-made terraces. These platforms were typically ∼8–10 m in diameter and were often used repeatedly (Knapp et al., 2015). In contrast, in regions with flat topography platforms could have been larger, with diameters of up to 30 m (Rösler et al., 2012; Raab et al., 2015). Depending on the size of the charcoal hearth, the pyrolysis process required up to 20 days. After cooling, the hearth was opened and the charcoal was raked out for harvesting. Typically, the residues of the charring process, such as small charcoal pieces, ash, and the material used to seal the charcoal hearth and burnt soil, remained on the platform and formed a new layer covering the former surface (Kemper, 1941; Bond, 2007; von Kortzfleisch, 2008).

From a pedological view, this layer associated with relict charcoal hearths (RCHs) can best be described as a technogenic or anthropogenic sedimentary deposit. The properties of this layer are fundamentally controlled by the effects of charring on the mineral and organic matter in the soil and the loose structure of the deposit. For instance, Borchard et al. (2014) reported that the substrates of RCHs have a lower bulk density than the topsoils outside of charcoal hearths. Mastrolonardo et al. (2018) recently reported that RCHs contribute up to 4.2 % carbon to the carbon stock in a Mediterranean forest. Furthermore, the soil below the wood stack is affected by heat during the pyrolysis process. Heat directly and indirectly influences the chemical, biological, mineralogical and physical properties of the soil (Certini, 2005; Mataix-Solera et al., 2011). Recent studies on plants growing on RCHs and pot experiments with RCH substrates suggest that the substrate influences vegetation via soil-plant interactions (Carrari et al., 2016; Criscuoli et al., 2017), while earlier studies found no indications for any long-lasting

effects for plant growth on RCHs despite more favorable soil conditions (Borchard et al., 2014). Although studies from North America and Europe report thousands of RCHs in modern forest ecosystems (Hesse, 2013; Johnson et al., 2015; Schmidt et al., 2016) and very high site densities (Raab A. et al., in press), questions remain regarding the classification of RCH soils, the effects of burning on soil properties and the subsequent pedogenesis. For instance, these soils are characterized by translocated soil material with further amendments, are mostly ignored in the German Guidelines for Soil Mapping (Ad-hoc-AG Boden, 2005), despite the wide distribution of RCHs in Germany. Hence, following the pedogenic approach of the German Soil Taxonomy, we aim to explore the main soil-forming processes in charcoal hearth soils by (i) characterizing the influence of burning on the inorganic and organic soil materials (hereinafter termed as "substrate") of RCHs, (ii) describing the characteristic features and properties of the associated soil horizons and (iii) discussing the classification according to the current German Guidelines for Soil Mapping. For this purpose, we combine a pedological survey with analyses of micromorphology and soil chemistry in a type region of historic charcoal production in South Brandenburg. We studied soils on two representative RCHs and compared these findings with the soil next to the RCHs and four typical soils on similar parent material located at distances between 10 and 70 km.

METHODS

Study Site and Fieldwork

We focus on two charcoal hearth sites (RCH 970 and RCH 1089) located ∼10 km east of the city of Peitz, Brandenburg, Germany (**Figure 1a**), where active open-cast lignite mining has prompted systematic, large-scale archeological excavations. In this area of a former historic forest district, archeological excavations (Rösler et al., 2012) in combination with GIS analyses (Raab et al., 2015; Raab A. et al., in press) have revealed the remains of more than 1200 RCHs that supplied charcoal to the historical ironworks in Peitz and other forest districts from the mid-sixteenth to the mid-nineteenth centuries (Müller, 2017). Although, the size and shape of the RCHs at the study site can vary slightly to some extent (Rösler et al., 2012), our two selected RCHs feature a characteristic architecture and soil stratigraphy. Thus, our studied RCHs are representative for the study site, and also for RCHs on flatland in Poland or Belgium (Hardy et al., 2016; Rutkiewicz et al., 2017). Dendrochronological analyses on charcoal residues from RCH 970 revealed that this charcoal hearth was constructed from trees that were felled from 1711 to 1721 (Raab A. et al., in press). Thus, the RCH 970 was abandoned ∼300 years ago. The RCHs are round platforms surrounded by shallow ditches. The remains of the charring process form mounds that are ∼30 cm thick on the platforms and partly fill the ditches (**Figure 1b**) (Raab et al., 2015). The ditches around the platforms have outer diameters of between 4 and 30 m, and most of the sites were used only once. The colliers mainly used Scots pine (*Pinus sylvestris* L.) for charring, as this was and still is the dominant tree species in the study area. The soil parent material of the study site is sandy glaciofluvial sediment deposited during
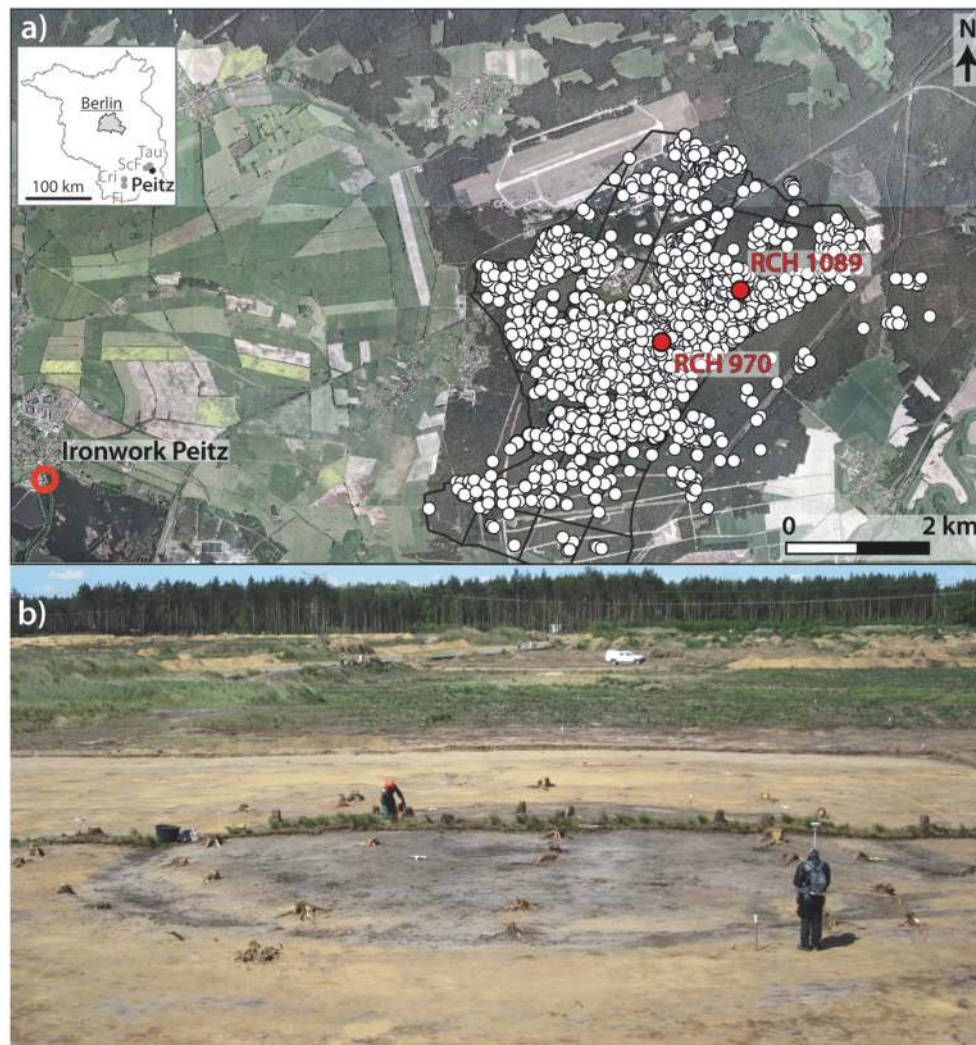
FIGURE 1 | (a) RCHs (white dots, map as of 2016) in the historic forest plots (black grids) east of the city of Peitz (orthophoto from 2005, Vattenfall Europe Mining AG/Lausitzer Energie Bergbau AG); Fi, Finsterwalde; ScF, Schmogrow-Fehrow; Tau, Tauer; Cri, Crinitz; **(b)** view looking west at charcoal hearth RCH 970 at the beginning of archeological excavation.

the Weichselian glaciation (Lippstreu et al., 2003). Brunification and podzolization are the dominant pedogenic processes in this sandy substrate (Bauriegel et al., 2015).

Our study site is situated in the forefield of the active lignite mine Jänschwalde. Before the area was logged and earthworks were conducted in preparation for mining, the study sites were cordoned off to prevent disturbances of the soil profiles by heavy machinery. The soil mapping and sampling were performed in north-south-oriented trenches passing through the centers of RCH 970 (soil profile RCH 970$_{in}$) and RCH 1089 (soil profile RCH 1089$_{in}$). To map the soil outside of the RCHs, another soil pit, RCH1089$_{out}$, which is located ~20 m NE of RCH 1089, was studied. The soils were described and classified according to the German Guidelines for Soil Mapping (Ad-hoc-AG Boden, 2005) and were also classified according to the WRB (IUSS Working Group WRB, 2014). Bulk samples were taken from each

mineral horizon in the three studied soil profiles. No samples were taken from the organic horizons (L/Of/Oh). Additional sampling was performed at RCH 970$_{in}$ from the topsoil to a depth of 112 cm with a high vertical resolution (5–7 cm) for ex situ measurements of magnetic susceptibility and elemental analysis via X-ray fluorescence.

Soil Analysis

Laboratory analyses were performed on air-dried and sieved (<2 mm) samples. Soil colors were assessed using a Munsell soil color chart (Munsell, 2009). Granulometry was performed via a combination of wet sieving and pipetting with 40-g sample aliquots and without H_2O_2 pretreatment (Deutsches Institut für Normung e.V., 2002). Soil pH was determined potentiometrically at the ratio of 1:2.5 in a 0.01 M $CaCl_2$ solution. Phosphorus was extracted in a parallel fashion with calcium-acetate-lactate (P_{CAL})

(VDLUFA, 2012) on 5 g of soil and measured using an ICP-OES (Thermo Fisher Scientific, ICAP, 6300 Duo).

The total carbon (C), nitrogen (N) and sulfur (S) concentrations were analyzed by gas chromatography on ground aliquots via high-temperature heating in an Elementar VARIO EL cube analyzer (Deutsches Institut für Normung e.V., 1996, 1998). The total Fe, Mn, Ca, K, and Pb concentrations were measured on aliquots via X-ray fluorescence with a Niton XLT3 analyzer. Magnetic susceptibility was determined ex situ using a Bartington MS3 magnetic susceptibility meter and a MS2B dual-frequency sensor in 10-ml flasks by measuring the susceptibility at 460 Hz. We measured the volumetric magnetic susceptibility (χ_v, in SI) and calculated the mass magnetic susceptibility (χ_{mass}, in SI) by noting the bulk density of each sample prior to the measurement. Undisturbed soil samples were collected in Kubiëna tins for thin section preparation. The thin sections of air-dried samples were prepared via impregnation with resin and subsequent cutting and grinding to 25 µm, following Beckmann (1997). The micromorphology was described according to Stoops (2003).

The soil data for the four soil profiles (Tauer, Crinitz, Schmogrow-Fehrow, and Finsterwalde) used for the comparison were kindly provided by the Geological State Service of Brandenburg. All of the analyses were performed using the same standard methods; however, a PW2400 PANalytical was used to perform the X-ray fluorescence measurements.

RESULTS
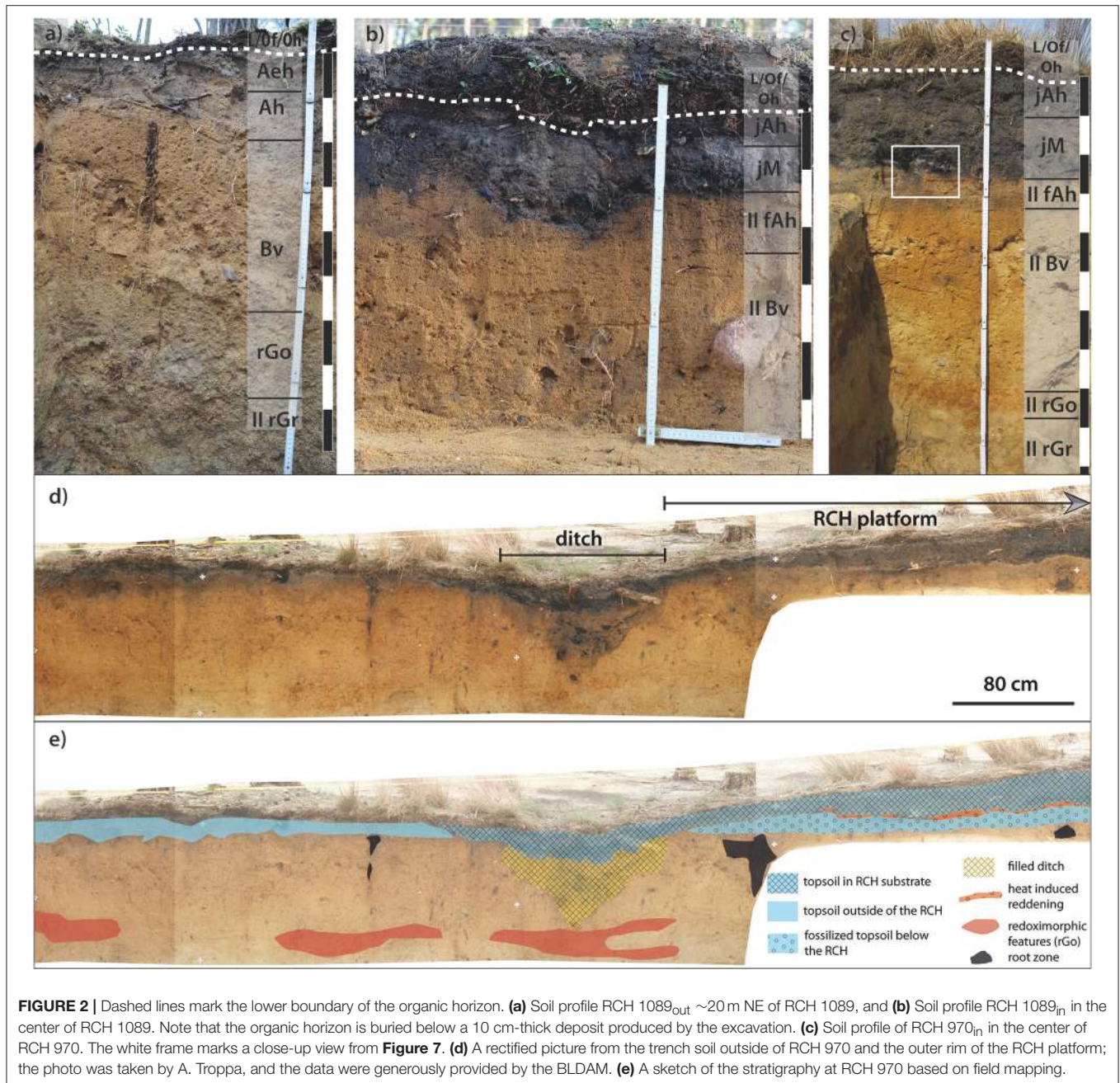
Natural Soil Formation

The dominating pedogenic processes in the sandy deposits of the study site are brunification and podzolization. The soil outside of the RCHs is a Podsolige Braunerde [WRB: Brunic Arenosol (Protospodic), **Figure 2a**] and the grain-size distribution of this soil is dominated by sand (**Table 1**). At a depth of 50 cm, the presence of ventifacts indicate periglacial processes and classifies the sediment as a coversand, which is a typical facies in the Northern German lowland (Kasse, 2002) and a widespread and characteristic deposit in our study area (**Tables 1**, **2**). The coversand has a thickness of 80 cm, and the texture is dominated by coarse and medium sand. The glaciofluvial deposits below are characterized by distinctively higher contents of gravel (20–200 mm). The topsoil has a brown-to-pale brown color and contains 10.9 g kg^{-1} C (**Table 1**). Hence, the topsoil's C concentration is characteristic of soils developed in the sandy substrate and under the dry and continental climate of Lower Lusatia in South Brandenburg (**Table 2**). The uppermost 9 cm of the topsoil are characterized by podzolic bleaching (**Figure 2a**, **Table 1**), but the eluvial horizon shows features of intermixing due to modern forest plowing or earlier prehistoric plowing (Schneider et al., 2016). In two of the four reference profiles (**Table 2**), the Pb concentration is slightly higher in the uppermost part of the topsoil of RCH 1089$_{out}$ than in the horizons below (**Table 1**). We associate this higher Pb concentration with the eolian deposition of air pollutants during the last decades.

Although an illuvial horizon could not be identified during the field survey, the striking increase in the total Fe concentration

to 8,828 mg kg^{-1} at depths between 18 and 32 cm indicates the translocation of Fe by podzolization. Furthermore, the micromorphological study of the thin sections from RCH 970$_{in}$ at that depth reveal the presence of yellowish iron oxide precipitates. This initial podzolization with the lack of an illuvial horizon is a characteristic feature of the soil development on the sandy substrates in Lower Lusatia (**Table 2**). Although the total Fe concentrations of the Bv-horizons of the soil profiles at Tauer and Schmogrow-Fehrow are remarkably higher than in the overlying horizons (**Table 2**), no morphological features of a Bs-horizon could be identified during the soil mapping. The total Fe concentration in these quartz-rich sediments are generally low and range between 2,300 and 4,300 mg kg^{-1} in the topsoil and subsoil, only exceeding 7,249 mg kg^{-1} in the Bs-horizon at Crinitz. The χ_{mass} of the non-fire affected topsoil at RCH 1089$_{out}$ ranges between 149 and 257 χ_{mass} 10^{-9} m^3 kg^{-1} (**Table 1**). The χ_{mass} of the non-fire affected substrate decreases with depth. Some outliers have been associated with magnetic minerals originating from the deposition of the sediment, such as in the parent material between 50 and 60 cm (RCH 970$_{in}$: χ_{mass} 254 10^{-9} m^3 kg^{-1}, **Table 1**), or pedogenic processes, such as in the redoximorphic horizons (rGo-horizon at RCH 1089$_{out}$: χ_{mass} 106 10^{-9} m^3 kg^{-1}, and rGo-horizon: χ_{mass} 26 10^{-9} m^3 kg^{-1}).

Soils on the Relict Charcoal Hearths

The studied hearths RCH 970 and RCH 1089 feature the characteristic architecture of RCHs on flatland, and 50-cm-wide ditches are present around the platforms (**Figure 1b**). At both sites, the remaining substrate layers of the RCHs have a thickness of ~30 cm (**Figures 2b,c**). The charcoal-bearing substrates of RCH 970$_{in}$ and RCH 1089$_{in}$ have a very dark gray-to-grayish brown color (**Table 1**), and their C concentrations range from 11.9 to 42.9 g kg^{-1}. Although we cannot differentiate between soil organic matter (SOM) and pyrogenic organic matter (PyOM; Knicker, 2011), the total C concentrations clearly differ between the soil outside of the RCHs and the RCHs' topsoils. The topsoils within the charcoal hearths (RCH 970$_{in}$: very dark gray and RCH 1089$_{in}$: dark grayish brown) contain approximately twice as much C$_T$ (23.0 g kg^{-1}, on average) as is present in the topsoil outside of the hearth sites (RCH 1089$_{out}$, brown), resulting in a strikingly darker color in the RCH topsoils because of their PyOM content (Eckmeier et al., 2007). Due to the enrichment in SOM, the uppermost 5 cm at RCH 1089$_{in}$ has a C concentration of 24.8 g kg^{-1}; while at a depth of 21 cm, the C concentration decreases to 11.9 g kg^{-1}. At the base of the RCH substrate (sample RCH 1089$_{in}$ in **Table 1**), the C concentration strikingly increases to 42.90 g kg^{-1}. The N concentration of both RCHs is ~0.5 g kg^{-1}, similar to RCH 1089$_{out}$ (**Table 1**) and the four reference soils (**Table 2**); the N concentration is higher (0.9 g kg^{-1}) only at the base of RCH 1089$_{in}$. We associate this increase with the input of young SOM from the roots. Remarkably, the S concentration (0.8–1.9 g kg^{-1}) of RCH 1089$_{in}$ is considerably greater than that of the topsoil at RCH 1089$_{out}$ or at RCH 970$_{in}$. The total concentrations of Ca, Mn and K are in the same range and have depth distributions that are similar to those of the soils outside of the RCHs (**Tables 1**, **2**).

FIGURE 2 | Dashed lines mark the lower boundary of the organic horizon. **(a)** Soil profile RCH 1089_{out} ~20 m NE of RCH 1089, and **(b)** Soil profile RCH 1089_{in} in the center of RCH 1089. Note that the organic horizon is buried below a 10 cm-thick deposit produced by the excavation. **(c)** Soil profile of RCH 970_{in} in the center of RCH 970. The white frame marks a close-up view from **Figure 7**. **(d)** A rectified picture from the trench soil outside of RCH 970 and the outer rim of the RCH platform; the photo was taken by A. Troppa, and the data were generously provided by the BLDAM. **(e)** A sketch of the stratigraphy at RCH 970 based on field mapping.

A sharp boundary separates the dark, carbon-rich substrates of the RCHs and the carbon-poor II fAh (**Figures 2b,c**). Due to the presence of black monomorphic organic matter and charred wood fragments in the substrates of the RCH, the striking boundary between the two substrates is also clearly visible in the thin sections. Textural features, such as the layering or orientation of sand grains, that might indicate truncation of the buried topsoil, were not detected at the boundaries between the RCHs and the II fAh or in other parts of the RCHs. The substrates of the RCHs are loose and contain scattered charred wood (**Figure 3a**) that ranges in size from stems to submicroscopic ($<20\,\mu$m). Furthermore, during the archeological excavations, black tarry chunks that are up to 10 cm in size (**Figure 3b**, termed "Brandschurf" in German; von Berg, 1860) were frequently found in the ditch surrounding the charcoal hearth platform. Moreover, the micromorphologic analysis also reveals that the sand grains found in the RCH substrate within $RCH970_{in}$ are partly cemented together into small aggregates by tarry material (**Figures 4a–d**). Under the microscope, the tarry material adhering to the sand grains is opaque under transmitted light and has a dull black color under incident light (**Figures 4b,c**). These tarlike compounds are

TABLE 1 | Soil parameters in the soil profiles of RCH 970$_{in}$, RCH 1089$_{in}$ and RCH 1089$_{out}$.

	Depth in cm	Soil color (dry sample)	Horizon	Substrate	Texture (Ad-hoc-AG Boden, 2005)	Sand in %	Silt in %	Clay in %	pH in CaCl$_2$	C	N	S (in g kg^{-1})	P$_{CAL}$ in mg kg^{-1}	χ mass in 10^{-9} m^3 kg^{-1}	χV in 10^{-6}	Fe in mg kg^{-1}	Ca in mg kg^{-1}	Mn in mg kg^{-1}	K in mg kg^{-1}	Pb in mg kg^{-1}
SOIL (PODSOLIGE BRAUNERDE) OUTSIDE OF RCH 1089																				
RCH1089$_{out}$	0–9	10YR 5/3	Aeh	pky-ss(Sp)	St2	88.2	6.5	5.3	3.6	10.90	0.50	0.10	3.83	149.2	222.2	6,233 ± 89	2,665 ± 97	72 ± 20	8,312 ± 197	36 ± 4
RCH1089$_{out}$	9–18	10YR 6/3	Ah	pky-ss(Sp)	St2	86.4	7.5	6.1	3.9	10.90	0.40	0.00	3.04	256.5	398.1	4,535 ± 76	1,972 ± 84	85 ± 20	6,933 ± 180	27 ± 4
RCH1089$_{out}$	18–32	10YR 7/6	Bv	pky-ss(Sp)	Ss(mSgs)	91.2	5.0	3.8	4.3	4.50	0.30	0.10	n.a.	119.5	204.3	8,828 ± 106	3,249 ± 108	152 ± 24	10,498 ± 222	17 ± 3
RCH1089$_{out}$	32–46	10YR 7/6	Bv	pky-ss(Sp)	Ss(mSgs)	92.3	3.7	4.0	4.3	3.00	0.20	0.00	n.a.	120.5	207.4	4,986 ± 78	2,242 ± 94	73 ± 20	8,703 ± 209	15 ± 3
RCH1089$_{out}$	46–60	10YR 7/6	Bv	pky-ss(Sp)	Ss(mSgs)	93.7	3.0	3.3	4.3	1.70	0.20	0.00	n.a.	94.7	162.4	4,422 ± 76	1,868 ± 83	28 ± 18	7,476 ± 185	15 ± 3
RCH1089$_{out}$	60–80	10YR 7/6	rGo	pky-ss(Sp)	Ss(mSgs)	95.2	2.0	2.8	4.4	1.10	0.20	0.20	n.a.	105.9	181.6	6,194 ± 88	2,014 ± 85	58 ± 20	7,220 ± 184	13 ± 3
RCH1089$_{out}$	80–100	10YR 7/5	II rGr	pky-ss(Ssdr)	Ss(mSgs)	97.4	0.5	2.1	4.2	0.80	0.20	2.70	n.a.	25.6	44.6	2,659 ± 59	1,408 ± 75	89 ± 20	7,003 ± 179	19 ± 3
RCH1089$_{out}$	100–113	10YR 7/4	II rGr	pky-ss(Ssdr)	Ss(mSgs)	97.0	1.0	2.1	4.3	1.10	0.20	1.40	n.a.	39.9	68.5	2,500 ± 57	1,669 ± 80	33 ± 18	6,244 ± 176	19 ± 3
RCH1089$_{out}$	113–120	10YR 8/4	II rGr	pky-ss(Ssdr)	Ss(mSgs)	98.4	0.2	1.3	4.4	0.50	0.10	0.60	n.a.	19.5	34.0	1,810 ± 49	1,242 ± 68	59 ± 18	5,097 ± 154	15 ± 3
SOIL IN THE CENTER OF RCH 1089 (KOLLUVIALE BRAUNERDE)																				
RCH 1089$_{in}$	0–5	10YR 5/2	jAh	uk-ss(oj), Bhk, X	Ss(mSgs)	91.0	4.5	4.6	3.5	24.80	0.70	1.90	4.71	918.2	1305.3	7,459 ± 97	2,724 ± 91	62 ± 20	7,881 ± 181	31 ± 4
RCH 1089$_{in}$	5–13	10YR 4/2	jM	uk-ss(oj), Bhk, X	Ss(mSgs)	93.0	3.5	3.5	4.0	16.30	0.40	1.10	4.95	956.1	1483.7	4,724 ± 77	2,086 ± 80	42 ± 18	6,515 ± 163	20 ± 3
RCH 1089$_{in}$	13–21	10YR 5/2	jM	uk-ss(oj), Bhk, X	Ss(mSgs)	94.8	2.2	3.0	4.3	11.90	0.40	1.00	3.75	1074.7	1701.9	5,272 ± 81	2,785 ± 94	122 ± 22	5,541 ± 162	20 ± 3
RCH 1089$_{in}$	21–23	10YR 5/2	jM	uk-ss(oj), Bhk, X	n.a.	n.a.	n.a.	n.a.	3.9	42.90	0.90	0.80	n.a.	461.1	719.6	4,164 ± 72	2,264 ± 90	47 ± 18	5,526 ± 169	25 ± 3
RCH 1089$_{in}$	23–31	8,75YR 6/4	II fAh	pky-ss(Sp)	Ss(mSgs)	92.1	3.8	4.1	4.4	4.50	0.30	0.80	0.97	277.7	466.5	7,447 ± 98	2,623 ± 99	104 ± 22	10,009 ± 217	26 ± 4
RCH 1089$_{in}$	31–50	10YR 7/6	II Bv	pky-ss(Sp)	Ss(mSgs)	93.7	3.3	3.1	4.5	1.70	0.20	0.60	n.a.	103.7	177.4	4,688 ± 77	1,385 ± 74	44 ± 18	5,117 ± 162	15 ± 3
RCH 1089$_{in}$	50–70	10YR 7/8	II Bv	pky-ss(Sp)	Ss(mSgs)	96.7	1.5	1.8	4.6	0.50	0.10	0.30	n.a.	44.9	78.8	3,860 ± 71	1,267 ± 80	< LOD < LOD	10,346 ± 224	17 ± 3
RCH 1089$_{in}$	70–90	10YR 8/4	III Cv	pky-ss(Ssdr)	Ss(mSgs)	97.4	0.5	2.1	4.7	0.70	0.20	0.30	n.a.	41.2	69.4	1,997 ± 51	1,692 ± 76	< LOD < LOD	5,256 ± 157	19 ± 3
RCH 1089$_{in}$	90–100	n.a.	III rGo	pky-ss(Ssdr)	n.a.	n.a.	n.a.	n.a.	5.5	0.60	0.20	0.20	n.a.	n.a.	n.a.	n.a.	n.a.	< LOD < LOD	n.a.	n.a.
SOIL IN THE CENTER OF RCH 970 (KOLLUVIALE BRAUNERDE)																				
RCH 970$_{in}$	0–24	10YR 3/1	jAh/jM	uk-ss(oj), Bhk, X	n.a.	n.a.	n.a.	n.a.	3.8	22.70	0.49	0.41	12.65	620.2	937.4	2,793 ± 60	2,042 ± 84	33 ± 18	4,591 ± 153	18 ± 3
RCH 970$_{in}$	24–28	10YR 4/1	jM	uk-ss(oj), Bhk, X	n.a.	n.a.	n.a.	n.a.	4.0	19.50	0.47	0.24	12.95	880.0	1346.1	4,436 ± 74	2,463 ± 93	146 ± 22	8,194 ± 195	23 ± 3
RCH 970$_{in}$	28–32	8,75YR 6/6	II fAh	pky-ss(Sp)	n.a.	n.a.	n.a.	n.a.	4.3	4.94	0.30	0.23	11.64	222.3	373.0	5,192 ± 81	2,298 ± 82	155 ± 23	8,229 ± 177	20 ± 3
RCH 970$_{in}$	32–40	10YR 6/4	II fAh	pky-ss(Sp)	n.a.	n.a.	n.a.	n.a.	4.4	3.98	0.23	0.18	n.a.	140.0	231.1	3,898 ± 71	1,867 ± 82	174 ± 23	6,902 ± 179	20 ± 3
RCH 970$_{in}$	40–50	10YR 7/4	II Bv	pky-ss(Sp)	n.a.	n.a.	n.a.	n.a.	4.6	2.18	0.21	0.26	n.a.	112.8	194.4	6,357 ± 89	2,415 ± 94	90 ± 21	8,670 ± 202	13 ± 3
RCH 970$_{in}$	50–60	10YR 7/4	II Bv	pky-ss(Sp)	n.a.	n.a.	n.a.	n.a.	4.6	1.56	0.23	0.09	n.a.	254.6	449.4	4,635 ± 78	1,910 ± 88	200 ± 25	7,941 ± 199	14 ± 3
RCH 970$_{in}$	60–70	10YR 7/5	II Bv	pky-ss(Sp)	n.a.	n.a.	n.a.	n.a.	4.6	0.96	0.18	0.02	n.a.	63.6	112.8	4,334 ± 74	1,871 ± 88	32 ± 18	8,655 ± 207	14 ± 3
RCH 970$_{in}$	70–80	10YR 8/4	II Bv	pky-ss(Sp)	n.a.	n.a.	n.a.	n.a.	4.7	0.49	0.18	0.00	n.a.	65.3	112.7	2,446 ± 57	1,321 ± 80	< LOD < LOD	11,830 ± 229	19 ± 3
RCH 970$_{in}$	80–90	10YR 7/4	II Bv	pky-ss(Ssdr)	n.a.	n.a.	n.a.	n.a.	4.8	0.79	0.20	0.00	n.a.	41.2	68.9	2,159 ± 54	1,564 ± 83	27 ± 17	9,149 ± 210	18 ± 3
RCH 970$_{in}$	90–100	10YR 6/6	II rGo	pky-ss(Ssdr)	n.a.	n.a.	n.a.	n.a.	4.8	0.52	0.15	0.04	n.a.	91.6	156.1	3,937 ± 73	959 ± 64	57 ± 19	5,694 ± 162	16 ± 3
RCH 970$_{in}$	100–110	10YR 8/2	III rGr	pky-ss(Ssdr)	n.a.	n.a.	n.a.	n.a.	4.8	0.29	0.16	2.63	n.a.	17.4	28.5	5,796 ± 85	1,056 ± 61	63 ± 19	5,190 ± 146	14 ± 3

TABLE 2 | Soil parameters from four representative soils at distances between 10 and 70 km.

Depth (cm)	Horizon	Substrate	Texture	Sand in %	Silt in %	Clay in %	pH in CaCl$_2$	C	N	S	Fe	Mn	Ca	K	Pb
			(Ad-hoc-AG Boden, 2005)					in g kg^{-1}			in mg kg^{-1}				
PODSOLIGE BRAUNERDE, TAUER, UTM: 33U 464546 5751788															
0–5	Aeh	pky-ss(Sgf)	Ss(mSfs)	92.0	5.0	3.0	3.8	14.7	0.5	0.4	3,243	70	772	6,949	28
5–12	Bv-Ah	pky-ss(Sgf)	Ss(mSfs)	93.4	4.1	2.5	4.5	7.0	0.3	0.4	3,418	101	836	7,339	17
12–55	Bv	pky-ss(Sgf)	Ss(mSfs)	93.1	5.3	1.6	4.4	1.6	0.3	0.4	4,327	85	972	7,347	14
55–70	Bv-ilCv	pky-ss(Sgf)	Ss(mSfs)	97.9	0.0	2.1	4.5	0.6	0.3	0.4	2,670	70	715	5,878	21
70–160	ilCv1	pky-ss(Sgf)	Ss(mSfs)	99.3	0.0	0.7	4.8	0.6	0.3	0.4	1,692	54	815	7,123	16
160–210	ilCv2	pky-ss(Sgf)	Ss(mSgs)	100.0	0.0	0.0	4.8	0.6	0.3	0.4	1,978	77	1058	8,974	19
BRAUNERDE PODSOL, CRINITZ, UTM: 33U 416111 5732371															
0–5	Ahe	pky-(kk4)ss(Sp)	Su2	84.7	13.3	2.0	3.1	9.8	0.3	0.4	2,551	39	422	5,454	13
5–20	Ahe	pky-(kk4)ss(Sp)	Ss(mSgs)	91.2	8.7	0.1	3.2	6.9	0.3	0.4	2,600	39	364	5,363	15
20–30	Bv-Bs	pky-(kk4)ss(Sp)	Ss(mSgs)	91.6	8.4	0.0	4.3	9.5	0.4	0.4	7,249	31	422	6,268	17
30–60	Bv	pky-(kk4)ss(Sp)	Ss(mSgs)	93.8	6.2	0.0	4.4	1.0	0.3	0.4	3,383	23	465	7,273	10
60–85	ilCv	pky-(kk4)ss(Sp)	Ss(mSgs)	93.5	6.5	0.0	4.2	0.9	0.3	0.4	2,712	31	357	6,940	10
85–150	fBbt-ilCv	pky-(kk4)ss(Sp)	Ss(mSgs)	93.7	4.8	1.5	4.0	0.6	0.3	0.4	2,936	23	293	6,459	17
STARK PODSOLIGE BRAUNERDE, SCHMOGROW-FEHROW, UTM: 33U 448095 5748353															
0–3	Ahe	pky-ss(Sp)	n.a.	n.a.	n.a.	n.a.	3.3	7.2	0.3	0.4	2,300	46	607	5,081	16
3–30	Bv	pky-ss(Sp)	Ss(mSfs)	93.0	7.0	0.0	4.2	4.4	0.3	0.4	4,033	62	658	5,720	11
30–50	Bv-ilCv	pky-ss(Sp)	Ss(mSfs)	96.9	0.0	3.1	4.3	1.0	0.3	0.4	2,642	62	593	5,438	7
50–120	fGo-ilCv	pky-ss(Sp)	Ss(mSfs)	99.2	0.0	0.8	4.6	0.6	0.3	0.4	1,810	70	700	5,728	10
RELIKTISCH VERGLEYTE PODSOL BRAUNERDE, FINSTERWALDE, UTM: 33U 414673 5723577															
0–2	Ahe	pky-ss(Sf)	Su2	89.1	10.9	0.0	3.4	16.4	0.6	0.4	4,292	54	672	5,587	30
2–10	Ah-Bsv	pky-ss(Sf)	Ss(mSfs)	91.7	8.3	0.0	4.2	6.6	0.3	0.4	4,229	62	636	5,288	13
10–30	Bv	pky-ss(Sf)	Ss(mSfs)	96.1	3.9	0.0	4.2	1.8	0.3	0.4	3,677	54	715	5,836	8
30–50	Bv-rGo	pky-ss(Sf)	Ss(mSfs)	98.4	1.6	0.0	4.5	0.8	0.3	0.4	2,097	39	515	5,421	5
50–75	rGro	pky-ss(Sf)	Ss(fSms)	95.1	4.9	0.0	4.6	0.6	0.3	0.4	1,377	39	507	5,529	5
75–130	rGr	pky-ss(Sf)	Ss(fSms)	94.9	5.1	0.0	4.9	0.6	0.3	0.4	951	31	364	4,633	5
130–200	Go	pky-ss(Sf)	Ss(mSfs)	98.2	0.0	1.8	4.8	0.6	0.3	0.4	1,328	31	415	3,985	5

Data kindly provided by the Landesamt für Bergbau, Geologie, und Rohstoffe Brandenburg.

byproducts of the charring of fresh and highly resinous wood at ~450 °C (Braadbaart and Poole, 2008).

The buried topsoils in the centers of both RCHs display a three-part appearance (**Figures 2, 7**). The upper 2 cm of the preserved topsoil (28–30 cm) has a reddish luster (**Table 1**), the substrate below is light yellowish brown and the soil at the base of the II fAh horizon has a pale brown color, similar to that of the topsoils seen in the soils outside. The micromorphology of the II fAh horizon between 28 and 33 cm is characterized by the presence of few charcoal fragments, recent roots, and sclerotia. Similar to the recent topsoil outside of the RCH, the II fAh has a granular structure (**Figures 4e,f**). Between 33 and 35 cm, the amount of charcoal fragments increases, and fungal hyphae and monomorphic organic matter are additionally present. The C concentrations of the buried topsoil at RCH 1089$_{in}$ (23–31 cm: 4.50 g kg^{-1}) and RCH 970$_{in}$ (28–40 cm: 3.98 to 4.94 g kg^{-1}) are lower than those in the recent topsoil at RCH 1089$_{out}$ (0–18 cm: 10.90 g kg^{-1}).

The soil pH in the Ah horizons ranges from pH 3.5–3.8 in the uppermost part of both studied RCHs and ranges from pH 4.0–4.3 in the lower horizons (**Table 1**). The substrates below both RCHs represented by their Bv horizons have slightly higher pH values (4.5–4.8). At both sites, the magnetic susceptibility is greater in the substrate of the RCHs (χ_V: 720 to 1,702 10^{-6} and χ_{mass}: 461 to 1,074 10^{-9} m^3 kg^{-1}, **Tables 1, 3**) than in the buried soil below (**Figure 5**).

Discussion—Impact of Charcoal Production on Soil Stratigraphy and Soil Properties

Although soils on the RCHs notably differ to the soils in their surroundings by soil stratigraphy and SOM concentrations, soil acidity is very similar between the RCHs and the topsoils outside. Similar pH values ranging from 3.8 to 4.1 have been reported for RCHs in the Siegerland (Borchard et al., 2014). The soil acidity in hearth substrates is close to neutral only on active or very young charcoal hearths (Hardy et al., 2016). Hence, a liming effect associated with the formation of CaCO$_3$ through the heating of plant material containing calcium oxalate (Graustein et al., 1977; Knicker, 2011) is probably not anymore discernible on our studied sites because of the age of the RCHs.

Although the RCH substrates contain dark areas with high charcoal contents as well as grayish sandy areas, we attribute
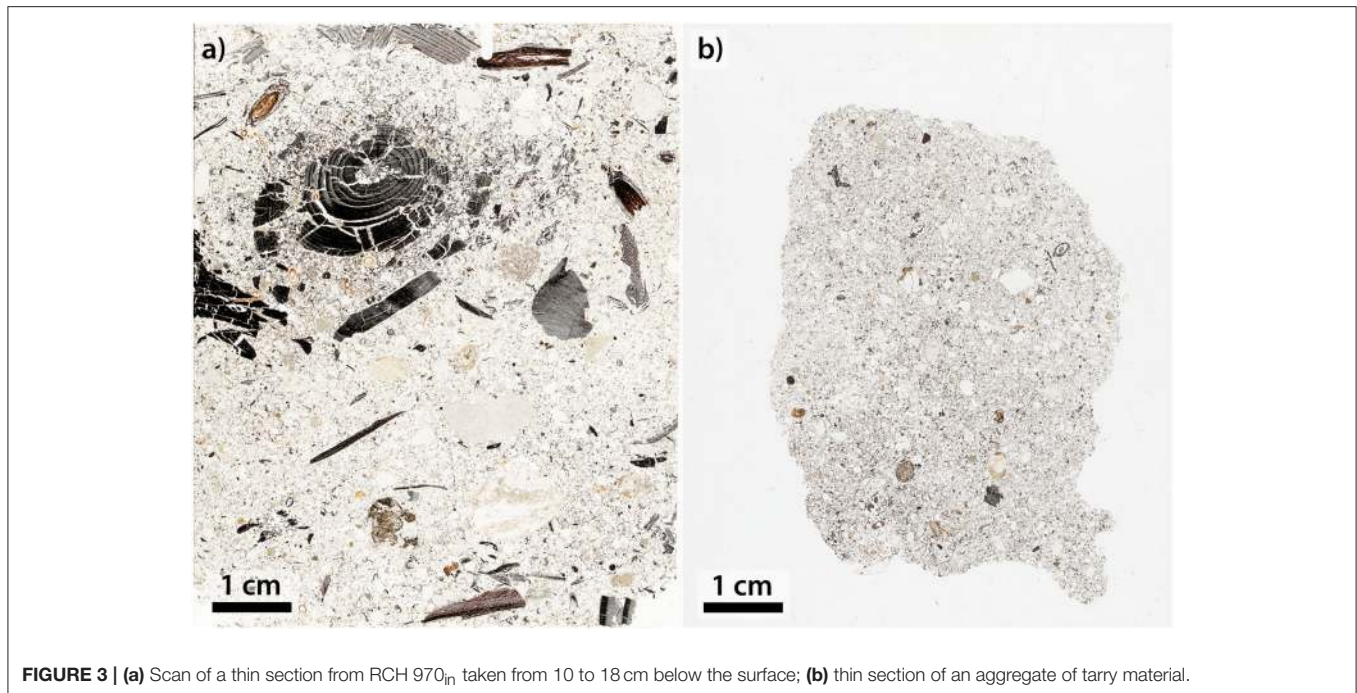
FIGURE 3 | (a) Scan of a thin section from RCH 970$_{in}$ taken from 10 to 18 cm below the surface; **(b)** thin section of an aggregate of tarry material.

this heterogeneous color of the RCHs to the complex formation of the substrates rather than pedogenic processes such as post-burn podzolization, considering the weak podzolization of the soil outside of the charcoal hearths. While the soil pH range of the RCHs favors podzolization, so far no illuvial features are identifiable in the thin sections of the RCH substrates or the substrates below the charcoal hearths. Also the total Fe concentration of the RCH sites also does not indicate podzolization-induced Fe translocation yet. Whereas podzolization in sandy substrate is notably by an enrichment of Fe in the subsoil after roughly 300 years (Burt and Alexander, 1996; Barrett, 2001), we attribute the lack of podzolization features on the RCHs so far to less annual precipitation than needed to cause podsolization within 300 years. Also, the reported lower bulk density of the RCHs substrate caused by the presence of SOM may retard podsolization by preventing the percolation of acidic soil solutions due to a higher water holding capacity of the SOM.

During the granulometric analysis, the dispersed topsoil samples from RCH 970$_{in}$ and RCH 1089$_{in}$ retained an intense black and opaque color in the sedimentation cylinders, even after they were allowed to settle for 1 day. The content of fine charcoal particles is not distinguishable and determinable via the standard granulometric method because the density of pine charcoal (true density: 1.38–1.46 g cm^{-3}, apparent density: 0.28 g cm^{-3}; Brocksiepe, 2000) is lower than the assumed density of 2.65 g cm^{-3} used in the calculation of the sedimentation time, and because the ratio of the organic fraction to the mineral fraction is very low. Hence, these observations strongly indicate that RCHs contain a high content of fine textured PyOM that needs to be considered in future studies due to high surface of small particles and their importance for pedological processes. Furthermore, the

topsoil of RCH 1089$_{in}$ has a higher sand content than the topsoil outside of the charcoal hearth (**Table 1**), which is reasonable because allochthonous material from the vicinity or the ditch surrounding the platform, presumably turf or material from B or C horizons, was usually used to cover and seal the wood stack prior to and during its operation. Furthermore, the royal Prussian order regulating forest logging and charcoal burning (Friedrich, 1779) advised the colliers to prevent any flaring of tar from the base of the charcoal hearth by throwing sand on the extinguished and uncovered charcoal hearth. The wet sieving of the coarse sand fraction of RCH 1089$_{in}$ (13–21 cm) reveals a notable amount of charred woody residues documenting an increasing charcoal concentration with depth. Charcoal contents increasing with depth in RCHs were also reported from Germany in the Black Forest and the Harz Mountains (Knapp et al., 2013; Quednau and Ludemann, 2017). These residues suggest that organic matter fell through the wood pile during the operation of the charcoal hearth and accumulated at its base or that ground vegetation or litter that had not been removed during the preparation of the hearth site became charred *in situ*. This again agrees well with the royal Prussian order regulating forest logging and charcoal burning. Friedrich (1779) ordered that the ground vegetation should not be removed at sandy sites because the charcoal pile would become unstable (§ 3: "[…] so muß der Köhler sich nach der Beschaffenheit jenes Ortes zu helfen suchen, und den auf diesem Sandboden befindlichen Rasen nicht abräumen, indem sich sonst das aufgesetzte Kohlenholz durch seine eigene Schwere eindrücken und auf einen Fuß tief nicht verkohlen würde."). Furthermore, in our north-south running trench, the lower half of the recent topsoil outside of RCH 1089$_{out}$ can be traced and connected with the buried topsoil under the charcoal hearth; the only interruption is the ditch surrounding
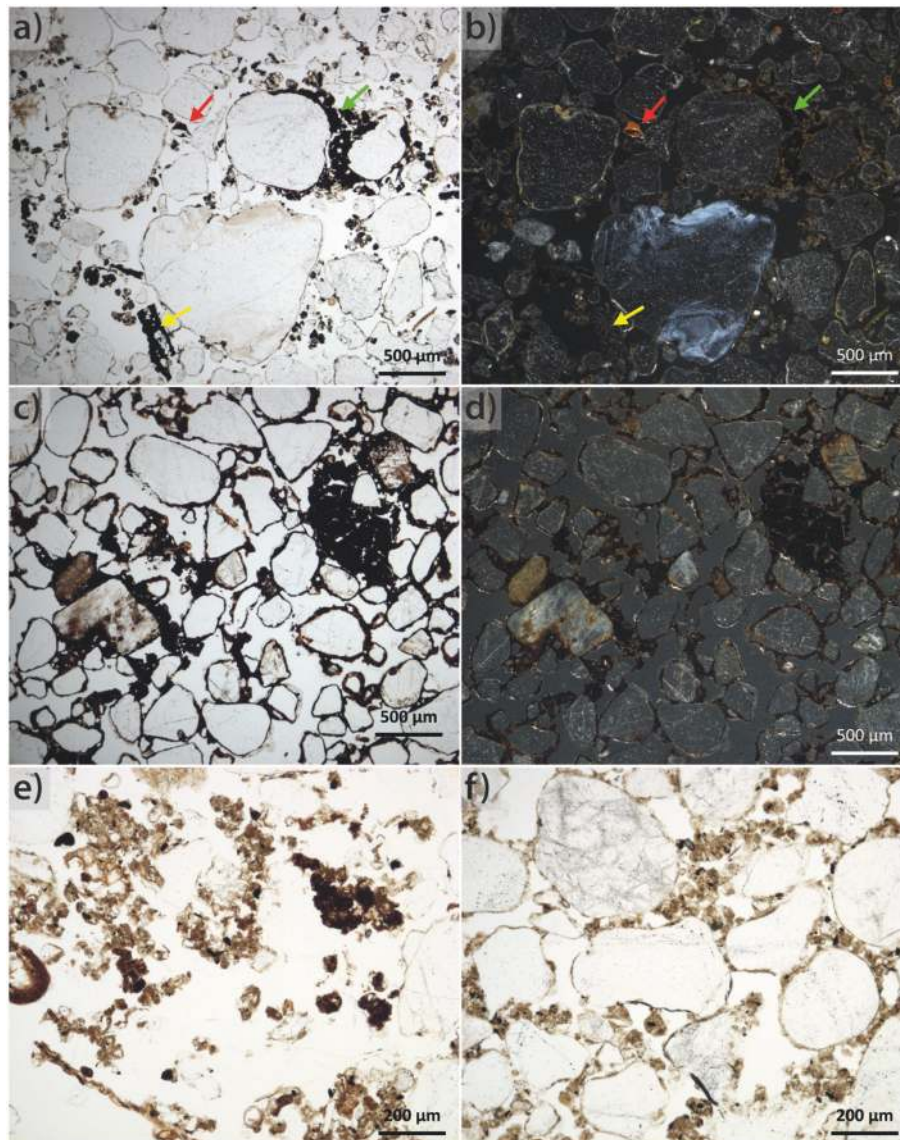
FIGURE 4 | Micrographs of a sample collected at a depth of 8 cm in the jAh horizon in RCH 970$_{in}$ made with **(a)** parallel; **(b)** oblique incident light. These micrographs show iron oxides (red arrows), charred wood (yellow arrows), and tar-like cements (green arrows). Micrographs from a specimen of massive sand with a diameter of 8 cm cemented with a tarlike substance taken from the ditch at RCH 970 under **(c)** linear polarization and **(d)** oblique incident light; **(e)** topsoil outside of RCH 970 and **(f)** from the II fAh with granular structure.

the RCH (**Figures 2d,e**). Therefore, the lack of site preparations at our studied RCHs due to the flatland together with the sandy soil might be a main contributor to differences with to RCHs in mid-mountain ranges, where there has been remarkable site preparation (Raab T. et al., 2017).

The contact zone that developed in the buried topsoil below the RCH substrate (**Figures 2c, 7**) is reddish in color, but this reddening is not continuous (**Figures 2d,e**). Either the conditions necessary for the formation of the reddish contact zone were not fulfilled, or the area was destroyed during the harvesting of the charcoal. The reddish color contradicts a podzolic illuvial genesis because Bs-horizons are dominated by goethite (Campbell and

Schwertmann, 1984) and therefore have a yellowish color. Furthermore, illuvial horizons, which are discernible by color, were not found outside of the RCHs in the field survey. The grains in the thin sections taken from the RCH substrates and from the contact zone between the charcoal hearth and the underlying soil have a red luster. The sand in the RCH substrates is primarily quartz, but some of the non-quartz mineral grains in the sand and silt fractions and in the clay adhering to the sand grains display a reddish luster. This reddening is accompanied by higher χ_{mass} in the RCH substrates and in a 2-cm-thick contact zone in the underlying buried soil (at a depth of 30 cm, **Figure 5**). The different soil colors that are noted in the buried

TABLE 3 | Magnetic susceptibility, soil color and Fe from the additional high vertical resolution sampling at RCH 970$_{in}$.

Depth in cm	Horizon	Substrate	Munsell color dry	Fe in mg kg^{-1}	χmass in 10^{-9} m^3 kg^{-1}	χv in 10^{-6}
		(Ad-hoc-AG Boden, 2005)				
0–3	jAh/jM	uk-ss(oj), Bhk, X	7.5YR 2.5/1	8,656 ± 104	708.8	894.1
3–10	jAh/jM	uk-ss(oj), Bhk, X	10YR 4/2	7,203 ± 96	585.3	768.4
10–17	jM	uk-ss(oj), Bhk, X	10YR 3.5/1	4,753 ± 77	619.8	809.2
17–21	jM	uk-ss(oj), Bhk, X	10YR 2.5/1	5,712 ± 85	704.2	958.7
21–25	jM	uk-ss(oj), Bhk, X	10YR 5.5/1	3,938 ± 71	556.6	868.5
25–26	jM	uk-ss(oj), Bhk, X	10YR 2/1	3,482 ± 67	802.3	1,224.7
26–28	II fAh	pky-ss(Sp)	6.25YR 6/3	5,673 ± 85	452.0	736.9
28–37	II fAh	pky-ss(Sp)	10YR 6/4	4,975 ± 80	133.8	204.3
37–43	II fAh	pky-ss(Sp)	10YR 7/3	4,281 ± 74	163.0	269.3
43–48	II Bv	pky-ss(Sp)	10YR 7/4	5,734 ± 85	216.2	361.7
48–53	II Bv	pky-ss(Sp)	10YR 6/4	3,935 ± 71	136.6	223.7
53–58	II Bv	pky-ss(Sp)	10YR 7/4	3,099 ± 64	91.7	159.1
58–63	II Bv	pky-ss(Sp)	10YR 7/5	5,133 ± 81	48.9	84.4
63–68	II Bv	pky-ss(Sp)	10YR 7/6	4,229 ± 73	60.4	100.1
68–73	II Bv	pky-ss(Sp)	10YR 7/6	2,448 ± 56	50.7	87.6
73–78	II Bv	pky-ss(Sp)	10YR 7/6	2,593 ± 58	46.2	77.1
78–83	II Bv	pky-ss(Sp)	10YR 7/4	2,893 ± 61	59.3	97.1
83–88	II Bv	pky-ss(Sp)	10YR 7/6	3,421 ± 66	65.1	110.4
88–93	II rGo	pky-ss(Ssdr)	7.5YR 7/6	2,753 ± 59	44.5	77.9
93–97	II rGo	pky-ss(Ssdr)	7.5YR 7/6	4,521 ± 74	52.9	88.8
97–102	III rGr	pky-ss(Ssdr)	10YR 8/3	2,100 ± 53	81.1	132.9
102–107	III rGr	pky-ss(Ssdr)	10YR 8/3	1,615 ± 47	44.2	70.3
107–112	III rGr	pky-ss(Ssdr)	10YR 8/3	1,326 ± 43	28.4	45.9

topsoils can be explained by thermally induced changes in soil properties. The reddish substrate in the upper 2 cm has a χ_{mass} of 452 10^{-9} m^3 kg^{-1} (**Figure 5**). However, in the light yellowish substrate below this depth, χ_{mass} decreases to 134–216 10^{-9} m^3 kg^{-1}. Thus, the soil color and the magnetic susceptibility measurements demonstrate that the transfer of heat into the mineral soil below the hearth during the charring process causes thermally induced recrystallization of iron (hydr-)oxides. Dupin et al. (2017) reported an χ_v between 600 and 1,100 10^{-6} for the RCH substrate from France; hence, the substrates of our studied RCHs have a similar range for their χ_v (χ_v: 720–1,702 10^{-6} and χ_{mass}: 461–1,074 10^{-9} m^3 kg^{-1}, **Tables 1**, **3**). Dupin et al. (2017) concluded that charcoal burning caused a doubling of χ_v over that observed in the non-fire affected substrate. However, the non-fire affected substrate in their study has a much higher χ_v (350–550 10^{-6}), whereas the non-fire affected substrate at our sites has a lower χ_v (<100–550 10^{-6}). Heat-induced reddening is caused by the dehydroxylation of iron hydroxides, which induces their direct recrystallization to hematite, although lepidocrocite transitions to maghemite in an intermediate phase (Cornell and Schwertmann, 2003). Depending on its degree of crystallinity, the recrystallization of goethite to hematite starts at a temperature of ∼260 °C (Schwertmann, 1984), that of lepidocrocite to maghemite starts above 200 °C, and that of maghemite to hematite begins within a range from 370 to 600 °C (Cornell and Schwertmann, 2003) (**Figure 6**). Temperatures within a charcoal hearth during the charring process range from

350 to 600 °C, but higher temperatures can be reached locally near the chimney (up to 750 °C) or when leakages occur (up to 1,100 °C) (Powell et al., 2012). Although the heat from the charring varies during the operation of charcoal hearths (Hollingdale et al., 1991), a temperature of ∼550 °C is maintained in charcoal hearths for at least several days, depending on the size of the hearth (Powell et al., 2012). The measurement of magnetic susceptibility can reveal the presence of the ferrimagnetic iron oxides maghemite and/or magnetite in RCH substrates (**Figure 5**) because magnetite and maghemite (480 and 380 kA m^{-1}) can achieve a higher saturation magnetization than goethite and hematite (2 and 2.5 kA m^{-1}) (Evans and Heller, 2003). In the presence of organic matter, goethite transforms to maghemite at temperatures between 370 and 600 °C (Schwertmann, 1985), and experimental approaches have demonstrated the presence of maghemite in fire-affected topsoils 16 h after burning (Nornberg et al., 2009). However, the post-burn formation of maghemite or magnetite in our studied profiles by microbial processes cannot be excluded (Maher, 1998). In addition, during the charring process, the iron-bearing minerals within charcoal hearths experience a reducing environment in the presence of carbon monoxide. The formation of metallic iron from iron hydroxides in association with carbon monoxide occurs after dehydration at temperatures below 300 °C (Jozwiak et al., 2007). Hematite can be transformed to metallic iron in this reducing environment. Hence, the chemical environment in the charcoal hearth favors the formation of metallic iron from iron oxides and iron
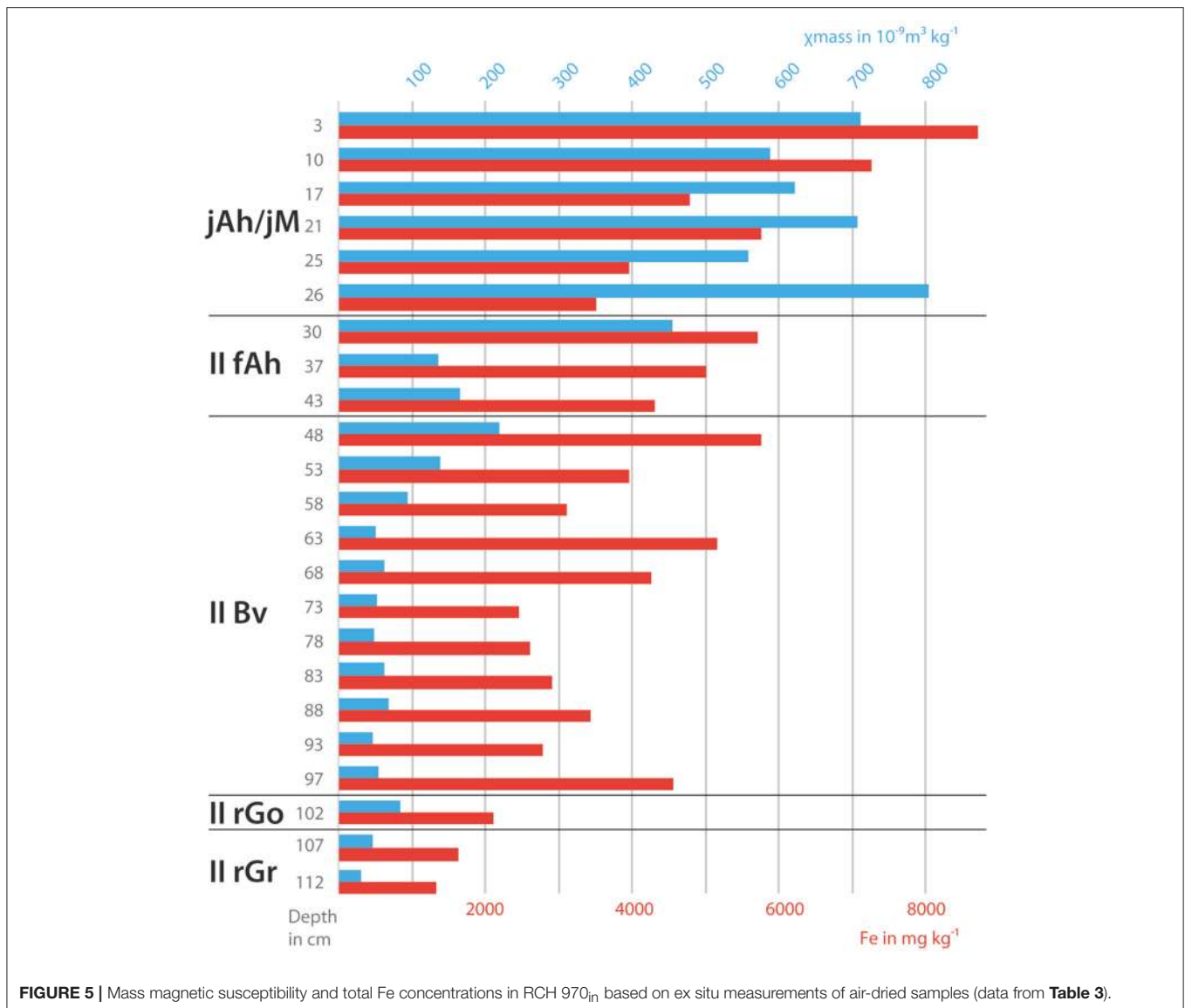
FIGURE 5 | Mass magnetic susceptibility and total Fe concentrations in RCH 970$_{in}$ based on ex situ measurements of air-dried samples (data from **Table 3**).

hydroxides. This finding is supported by comparisons between (pre-)historic hearth remains and reconstructed experimental fires in which a change in soil color directly below the hearth was detected and associated with post-fire pedogenic processes (Liedgren et al., 2017). Consequently, because a temperature of 350 °C is necessary to reset the optically stimulated luminescence (OSL) signal from quartz grains in the substrate of the hearth, the heat resulting from the operation of the charcoal hearth should be high enough to allow a successful dating of the RCH site by OSL (Armitage and King, 2013). Hence, the dating of the RCH operation by OSL might be a possibility in the absence of large enough charcoal pieces for dendrochronology or if radiocarbon dating is limited due to the ^{14}C-plateau.

However, these thermally induced changes in soil properties are restricted to a 2-cm-thick contact zone at a profile depth of 28–30 cm. Below this zone, in the underlying few centimeters of the profile and at depths of 30–33 cm, the temperature was too low to transform the iron(hydr-)oxides; however, it was

sufficiently high to cause the combustion of SOM, as indicated by the lighter color. No indication of the combustion of SOM was found below a depth of 33 cm. The combustion of SOM depends on its chemical structure and begins at 210 °C. At 450 °C, almost all SOM is combusted (Giovannini and Lucchesi, 1997). In a sandy-loamy topsoil beneath a fireplace described by Fenn et al. (1976), ~88 % of the SOM in the uppermost 2.5 cm of the soil was combusted, whereas only 45 % of the SOM from 2.5 to 7.5 cm was combusted. Experimental studies of heat transfer from fires into the underlying soils have shown that pore spaces act as a heat shield (Aldeias et al., 2016). Furthermore, ash and organic matter can also reduce the transfer of heat from fires into soils. When a sandy soil overlain by a 2-cm-thick layer of ash is heated, a surface temperature of 600 °C results in temperatures of ~400 °C at a depth of 2 cm and ~220 °C at a depth of 6 cm (Aldeias et al., 2016). Moreover, the presence of soil moisture below an active charcoal hearth hampers the transfer of heat into the soil (Powell et al., 2012; Brodard et al., 2016). We attribute the lack
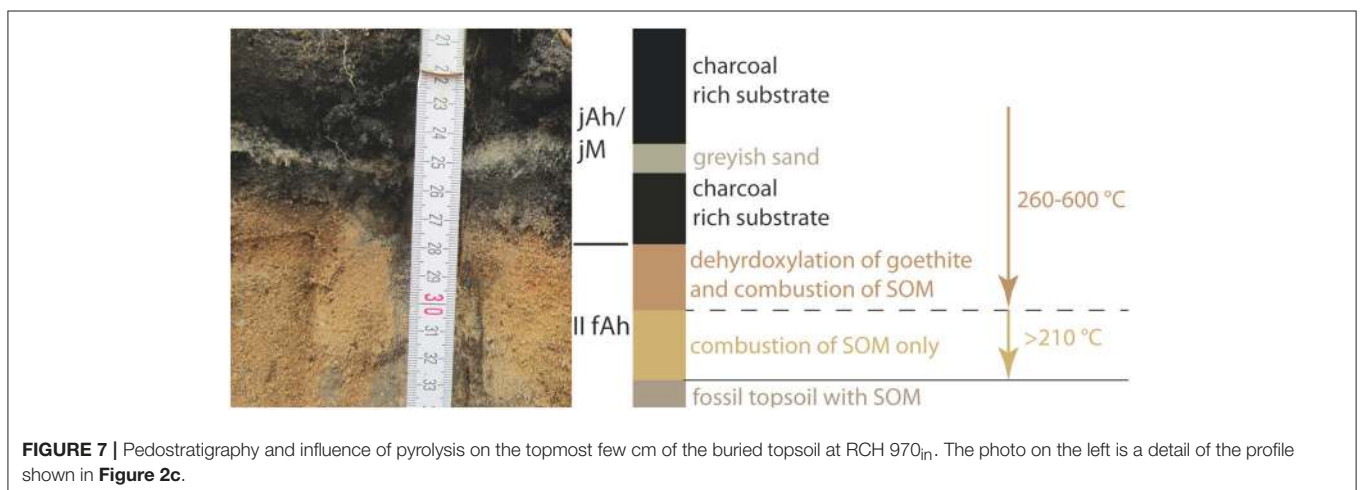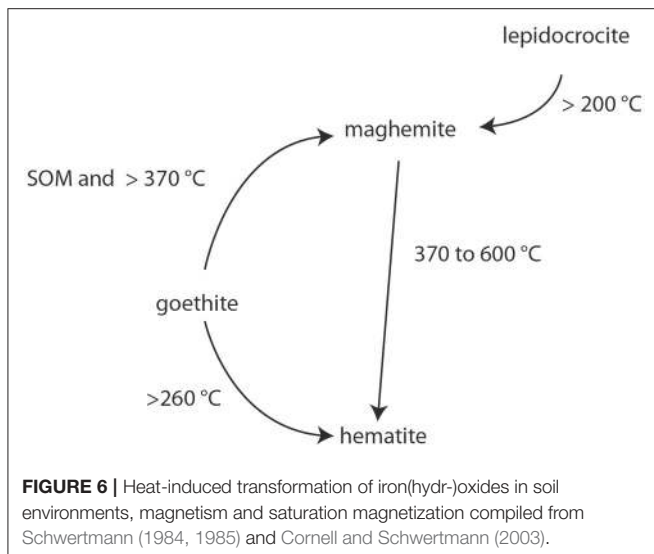
of SOM in the II fAh horizon between 30 and 33 cm depth to *in situ* combustion related to the heat of the pyrolysis occurring in the charcoal hearth above. Our micromorphological analysis shows no signs of the translocation of charred SOM from the charcoal hearths to the II fAh horizons like that reported for forest fires or fireplaces (Fenn et al., 1976; Gebhardt, 2007). The II fAh horizons contain mainly amorphous SOM, as well as some charred plant fragments, but the SOM and pyrogenic organic matter are evenly distributed in the fine soil. Additionally, no enrichment in SOM or pyrogenic organic matter is detectable in previously identified accumulation zones, such as those near the contact points between sand grains.

Synthesis: Soil Formation, Soil Properties, and Their Relation to Soil Classification Systems

The architecture of the RCH, the soil stratigraphy outside of the RCH, and our laboratory analysis suggest that the colliers

FIGURE 6 | Heat-induced transformation of iron(hydr-)oxides in soil environments, magnetism and saturation magnetization compiled from Schwertmann (1984, 1985) and Cornell and Schwertmann (2003).

placed the wood stock atop an undisturbed soil profile without mechanical preparation of the site with spades or hoes. During the operation of the charcoal hearth, the topsoil below was affected by the heat from pyrolysis, causing an alteration in the minerals and a combustion of the SOM. The magnetic susceptibility of the RCH is higher than that in the non-fire affected substrate below, and the reddish color of the substrate suggests a thermal alteration on the contact zone between the RCH and the soil below. Because the RCHs in our study area were in use between the mid-sixteenth and the mid-nineteenth centuries, the dendrochronological dating of the charcoal suggested that 1721 was the year of operation for RCH 970 (Raab A. et al., in press), and no indications for a later reuse were found, the maximum time during which soil formation occurred on RCH 970 is ca. 300 years.

The soils within both RCHs can be classified according to the German Guidelines for Soil Mapping as Regosol above Braunerde (jAh/jilC/II fAh/II Bv). However, the anthropogenic origins and the inherited and new chemical and physical characteristics of these soil sediments (jilC) are ignored in this classification. In an earlier (3rd) edition of the German Guidelines for Soil Mapping (Boden, 1982), "jY" was used to classify anthropogenic non-erosive relocated natural substrates, but this category was abandoned in later editions. Because "Y" is now used to indicate soil horizons formed by reductive gases, we suggest adapting the "M" horizon of the German Guidelines for Soil Mapping to allow a jM horizon. The implementation of a jM horizon would consider the anthropogenic raised charcoal content and indicate the anthropogenic nature (non-erosive translocated soil substrate) of this sediment. Thus, the soils within the RCHs would be classified as a Kolluviale Braunerde because the jM horizon is <40 cm thick. According to the WRB, which includes anthropogenic soil classifications, the soils on our studied charcoal hearths are classified as Spolic Technosols (Arenic) because the diagnostic criteria of >20 vol. % for artifacts is fulfilled by the low apparent density of the charcoal. Furthermore, the presence of anthropogenic charcoal allows the identification of a pretic horizon (IUSS Working Group WRB, 2014). However, because the substrate of the RCHs contains less than the required

FIGURE 7 | Pedostratigraphy and influence of pyrolysis on the topmost few cm of the buried topsoil at RCH 970$_{in}$. The photo on the left is a detail of the profile shown in **Figure 2c**.

P_{CAL} of 30 mg kg^{-1} (**Table 1**), the diagnostic criteria for the pretic horizon is nowhere near fulfilled for RCH 1089$_{in}$ (P_{CAL}: 3.75–4.95 mg kg^{-1}) and RCH 970$_{in}$ (P_{CAL}: 11.64–12.95 mg kg^{-1}). When phosphorus is extracted with Mehlich 1 (IUSS Working Group WRB, 2014) instead of CAL, the extractable phosphorus concentrations might have been slightly higher (Mylavarapu et al., 2002; Wuenscher et al., 2015). A classification of our two studied RCHs as Anthrosols analogs to the so-called "Terra Preta de Indio" (Glaser et al., 2000) fails to meet the diagnostic criteria of the WRB for Anthrosols. Hence, the presence of industrial-scale produced charcoal classifies the charcoal hearth soils as Technosols.

CONCLUSIONS

The architecture of our studied RCH sites indicates that due to the flatland topography together with a sandy soil, the operation of the RCH clearly differs from that in the mid-mountain ranges, where on slopes remarkable platform preparation and material movements has taken place.

Although the stratigraphy and the coloration of the RCH soils suggest the development of pedogenic horizons, we found no indication of pedogenic translocation or transformation processes besides the enrichment of PyOM in the substrate of the RCHs and decomposition of SOM below the RCHs by combustion. Due to the lack of data on the chemical properties of the RCH substrates immediately after the charring process, we cannot exclude the possibility that volatile compounds have been turned over and/or discharged since the operation of the RCHs and today. However, as we found no indications of the formation of pedogenic horizons, we suggest that, due to the young age of the RCHs, together with the sandy texture and the warm and temperate climate, soil development on the RCHs is still incipient. Thus, the technic character of the substrate is dominant.

Though pyrolysis occurs over the course of several days in charcoal hearths, the temperatures at which the soil mineralogy was visibly affected (∼400 °C) were limited to approximately the upper 2 cm of the soils in our study, and the combustion of SOM (which occurs at temperatures >220 °C) reached depths of ∼5 cm in the sandy soil below the charcoal hearths. Due to the heating of the substrate, it might be possible to date the RCH operation by OSL in the absence of large enough charcoal pieces for dendrochronology or if radiocarbon dating is limited due to the ^{14}C-plateau.

The studied charcoal hearths contain 23.0 g kg^{-1} C on average, approximately twice as much the studied topsoil outside of the charcoal hearths (10.9 g kg^{-1}). The charcoal that is present in the RCH substrates occurs in a wide range of grain sizes, from large fragments up to two decimeters in size to particles that are finer than sand. Because the specific surface area of these charcoal pieces affects soil chemistry and soil processes, further studies are required to examine the grain-size distribution of the charred organic matter and its chemical characteristics.

Even though charcoal hearths are common and widespread in Germany, the soils at these sites are rarely considered in terms of pedology, especially on soil maps and in soil taxonomic systems. Although the German Guidelines for Soil Mapping are designed to classify soils according to pedogenetic processes, the lack of a soil class for technic substrates and the minimum horizon thickness of 40 cm required to classify a soil as a Kolluvisol considerably hinder the classification of soils developed from anthropogenic sediments, such as charcoal hearths. The classification of soils in charcoal hearths as Spolic Technosols (Arenic) according to the WRB takes into account the anthropogenic genesis and the technic character of the substrate, which clearly distinguish these soils from the surrounding soils. Therefore, we suggest restating the diagnostic criteria of the M horizon in the German Guidelines for Soil Mapping to allow the classification of SOM-rich soil sediments as jM to Kolluvisol.

REFERENCES

Ad-hoc-AG Boden (2005). *Bodenkundliche Kartieranleitung.* Hannover: Bundesanstalt für Geowissenschaften und Rohstoffe.

Aldeias, V., Dibble, H. L., Sandgathe, D., Goldberg, P., and McPherron, S. J. P. (2016). How heat alters underlying deposits and implications for archaeological fire features: a controlled experiment. *J. Archaeol. Sci.* 67, 64–79. doi: 10.1016/j.jas.2016.01.016

Armitage, S. J., and King, G. E. (2013). Optically stimulated luminescence dating of hearths from the Fazzan Basin, Libya: a tool for determining the timing

and pattern of Holocene occupation of the Sahara. *Q. Geochronol.* 15, 88–97. doi: 10.1016/j.quageo.2012.10.002

Barrett, L. R. (2001). A strand plain soil development sequence in Northern Michigan, USA. *Catena* 44, 163–186. doi: 10.1016/S0341-8162(00)00170-3

Bauriegel, A., Pickert, E., Kühn, D., Krug, D., Eberhardt, E., and Stegger, U. (2015). *Bodenübersichtskarte 1:200.000 Cottbus CC 4750.* Hannover: Bundesanstalt für Geowissenschaften und Rohstoffe.

Beckmann, T. (1997). "Präparation bodenkundlicher Dünnschliffe für mikromorphologische Untersuchungen," in *Hohenheimer Bodenkundliche Hefte Stuttgart,* ed K. Stahr (Stuttgart: University Of Hohenheim), 89–105.

Boden, A. G. (1982). *Bodenkundliche Kartieranleitung*. Hannover: Bundesanstalt für Geowissenschaften und Rohstoffe und Geologische Landesämter.

Bolognesi, M., Vrieling, A., Rembold, F., and Gadain, H. (2015). Rapid mapping and impact estimation of illegal charcoal production in southern Somalia based on WorldView-1 imagery. *Energy Sustain. Dev.* 25, 40–49. doi: 10.1016/j.esd.2014.12.008

Bond, J. (2007). "Medieval charcoal-burning in England," in *Arts and Crafts in Medieval Rural Environment,* eds J. Klapste and P. Sommer (Szentendre: Brepols Publishers), 277–294. doi: 10.1484/M.RURALIA-EB.3.1147

Borchard, N., Ladd, B., Eschemann, S., Hegenberg, D., Möseler, B. M., and Amelung, W. (2014). Black carbon and soil properties at historical charcoal production sites in Germany. *Geoderma* 232–234, 236–242. doi: 10.1016/j.geoderma.2014.05.007

Braadbaart, F., and Poole, I. (2008). Morphological, chemical and physical changes during charcoalification of wood and its relevance to archaeological contexts. *J. Archaeol. Sci.* 35, 2434–2445. doi: 10.1016/j.jas.2008.03.016

Brocksiepe, H.-G. (2000). *Charcoal: Ullmann's Encyclopedia of Industrial Chemistry*. Weinheim: Wiley-VCH Verlag GmbH & Co. KGaA. doi: 10.1002/14356007.a06_157

Brodard, A., Lacanette-Puyo, D., Guibert, P., Lévêque, F., Burens, A., and Carozza, L. (2016). A new process of reconstructing archaeological fires from their impact on sediment: a coupled experimental and numerical approach based on the case study of hearths from the cave of Les Fraux (Dordogne, France). *Archaeol. Anthropol. Sci.* 8, 673–687. doi: 10.1007/s12520-015-0250-7

Burt, R., and Alexander, E. B. (1996). Soil development on moraines of Mendenhall Glacier, southeast Alaska. 2. Chemical transformations and soil micromorphology. *Geoderma* 72, 19–36.

Campbell, A. S., and Schwertmann, U. (1984). Iron oxide mineralogy of placic horizons. *J. Soil Sci.* 35, 569–582. doi: 10.1111/j.1365-2389.1984.tb00614.x

Carrari, E., Ampoorter, E., Bottalico, F., Chirici, G., Coppi, A., Travaglini, D., et al. (2017). The old charcoal kiln sites in Central Italian forest landscapes. *Quat. Int.* 458, 214–223. doi: 10.1016/j.quaint.2016.10.027

Carrari, E., Ampoorter, E., Verheyen, K., Coppi, A., and Selvi, F. (2016). Former charcoal kiln platforms as microhabitats affecting understorey vegetation in Mediterranean forests. *Appl. Veget. Sci.* 19, 486–497. doi: 10.1111/avsc.12238

Certini, G. (2005). Effects of fire on properties of forest soils: a review. *Oecologia* 143, 1–10. doi: 10.1007/s00442-004-1788-8

Chidumayo, E. N., and Gumbo, D. J. (2013). The environmental impacts of charcoal production in tropical ecosystems of the world: a synthesis. *Energy Sustain. Dev.* 17, 86–94. doi: 10.1016/j.esd.2012.07.004

Cornell, R. M., and Schwertmann, U. (2003). *The Iron Oxides Structure, Properties, Reactions, Occurences and Uses*. Weinheim: Wiley-VCH.

Criscuoli, I., Baronti, S., Alberti, G., Rumpel, C., Giordan, M., Camin, F., et al. (2017). Anthropogenic charcoal-rich soils of the XIX century reveal that biochar leads to enhanced fertility and fodder quality of alpine grasslands. *Plant Soil* 411, 499–516. doi: 10.1007/s11104-016-3046-3

Deforce, K., Boeren, I., Adriaenssens, S., Bastiaens, J., De Keersmaeker, L., Haneca, K., et al. (2013). Selective woodland exploitation for charcoal production. A detailed analysis of charcoal kiln remains (ca. 1300–1900 AD) from Zoersel (northern Belgium). *J. Archaeol. Sci.* 40, 681–689. doi: 10.1016/j.jas.2012.07.009

Deutsches Institut für Normung e.V. (1996). *DIN ISO 10694 Bestimmung von organischem Kohlenstoff und Gesamtkohlenstoff nach trockener Verbrennung (Elementanalyse): Bodenbeschaffenheit*. Berlin: Beuth Verlag.

Deutsches Institut für Normung e.V. (1998). *DIN ISO 13878 Bestimmung des Gesamt-Stickstoffs durch trockene Verbrennung (Elementaranalyse): Bodenbeschaffenheit*. Berlin: Beuth Verlag.

Deutsches Institut für Normung e.V. (2002). *ISO 11277: Verfahren mittels Siebung und Sedimentation Bodenbeschaffenheit - Bestimmung der Partikelgrößenverteilung in Mineralböden*.

Dupin, A., Girardclos, O., Fruchart, C., Laplaige, C., Nuninger, L., Dufraisse, A., et al. (2017). Anthracology of charcoal kilns in the forest of Chailluz (France) as a tool to understand Franche-Comte forestry from the mid-15th to the early 20th century AD. *Quat. Int.* 458, 200–213. doi: 10.1016/j.quaint.2017.03.008

Eckmeier, E., Gerlach, R., Skjemstad, J. O., Ehrmann, O., and Schmidt, M. W. I. (2007). Only small changes in soil organic carbon and charcoal concentrations found one year after experimental slash-and-burn in a temperate deciduous forest. *Biogeosci. Discuss.* 4, 595. doi: 10.5194/bgd-4-595-2007

Evans, M. E., and Heller, F. (2003). *Environmental Magnetism: Principles and Applications of Enviromagnetics*. Amsterdam; Boston, MA: Academic Press.

Fenn, D. B., Gogue, J. G., and Burge, R. E. (1976). *Effects of Campfires on Soil Properties*. Washington, DC: U.S. Department of the Interior.

Friedrich, P. K. II. (1779). *Verordnung, Wie es mit dem Holzschlag zu Kohlen und Köhlereyen bei den Königlichen Eisen= Blech= Kupfer= und Auch Anderen Hütten= und Hammerwerken Gehalten Werden Soll*. De Dato Berlin. Brandenburgisches Landeshauptarchiv, Pr. Br. Rep. 2A III F Regierung Potsdam, Holzkohlen-S. Kohlenschwelen in den kgl. Forsten und Holzschlag für Köhlereien bei den kgl. Hütten- und Hammerwerken (1738-1849), F.5-12.

Gebhardt, A. (2007). Impact of charcoal production activities on soil profiles: the micromorphological point of view. *ArcheoSciences* 31, 127–136. doi: 10.4000/archeosciences.833

Giovannini, G., and Lucchesi, S. (1997). Modifications induced in soil physico-chemical parameters by experimental fires at different intensities. *Soil. Sci.* 162, 479–489. doi: 10.1097/00010694-199707000-00003

Glaser, B., Balashov, E., Haumaier, L., Guggenberger, G., and Zech, W. (2000). Black carbon in density fractions of anthropogenic soils of the Brazilian Amazon region. *Org. Geochem.* 31, 669–678. doi: 10.1016/S0146-6380(00)00044-9

Graustein, W. C., Cromack, K., and Sollins, P. (1977). Calcium oxalate: occurrence in soils and effect on nutrient and geochemical cycles. *Science* 198, 1252–1254. doi: 10.1126/science.198.4323.1252

Groenewoudt, B. (2007). "Charcoal burning and landscape dynamics in the Early Medieval Netherlands," in *Arts and Crafts in Medieval Rural Environments,* eds J. Klapste and P. Sommer (Szentendre: Brepols), 327–333.

Hardy, B., Cornelis, J. T., Houben, D., Lambert, R., and Dufey, J. E. (2016). The effect of pre-industrial charcoal kilns on chemical properties of forest soil of Wallonia, Belgium. *Eur. J. Soil Sci.* 67, 206–216. doi: 10.1111/ejss.12324

Hesse, R. (2013). *Charcoal Burning Platforms in the Southern Black Forest: from LIDAR Point Cloud to Spatial Patterns of Resource Use*. Socio-environmental dynamics over the last 12,000 years: the creation of landscapes III. Kiel: Kiel University.

Hollingdale, A. C., Krishnan, R., Robinson, A. P., Institute, N. R., and Council, C. S. (1991). *Charcoal Production: A Handbook*. Prepared and produced for the Commonwealth Science Council by Natural Resources Institute. doi: 10.14217/9781848594876-en

IUSS Working Group WRB (2014). *World Reference Base for Soil Resources 2014*. FAO, Rome, 181.

Johnson, K. M., Ouimet, W., and Raslan, Z. (2015). *Geospatial and LiDAR-Based Analysis of 18th to Early 20th Century Timber Harvesting and Charcoal Production in Southern New England: Geological Society of America Northeastern Section Meeting: Bretton Woods*. New Hampshire, 65.

Jozwiak, W. K., Kaczmarek, E., Maniecki, T. P., Ignaczak, W., and Maniukiewicz, W. (2007). Reduction behavior of iron oxides in hydrogen and carbon monoxide atmospheres. *Appl. Catal. A Gen.* 326, 17–27.

Kasse, C. (2002). Sandy aeolian deposits and environments and their relation to climate during the Last Glacial Maximum and Lateglacial in northwest and central Europe. *Prog. Physical Geogr.* 26, 507–532. doi: 10.1191/0309133302pp350ra

Kemper, J. (1941). *American Charcoal Making in the Era of the Cold-Blast Furnace*. United Stated Dept. of the interior, National park service, Washington, DC, 1–25.

Knapp, H., Nelle, O., and Kirleis, W. (2015). Charcoal usage in medieval and modern times in the Harz Mountains Area, Central Germany: wood selection and fast overexploitation of the woodlands. *Quat. Int.* 366, 51–69. doi: 10.1016/j.quaint.2015.01.053

Knapp, H., Robin, V., Kirleis, W., and Nelle, O. (2013). Woodland history in the upper Harz Mountains revealed by kiln site, soil sediment and peat charcoal analyses. *Quat. Int.* 289, 88–100. doi: 10.1016/j.quaint.2012.03.040

Knicker, H. (2011). Pyrogenic organic matter in soil: its origin and occurrence, its chemistry and survival in soil environments. *Quat. Int.* 243, 251–263. doi: 10.1016/j.quaint.2011.02.037

Krebs, P., Pezzatti, G. B., Stocker, M., Bürgi, M., and Conedera, M. (2017). The selection of suitable sites for traditional charcoal production: ideas and practice in southern Switzerland. *J. Hist. Geogr.* 57, 1–16. doi: 10.1016/j.jhg.2017.04.002

Liedgren, L., Hörnberg, G., Magnusson, T., and Östlund, L. (2017). Heat impact and soil colors beneath hearths in northern Sweden. *J. Archaeol. Sci.* 79, 62. doi: 10.1016/j.jas.2017.01.012

Lippstreu, L., Sonntag, A., Horna, F., Badura, J., and Przybylski, B. (2003). *Geologische Übersichtskarte CC 4750 Cottbus*. Hannover: Bundesanstalt für Geowissenschaften und Rohstoffe.

Maher, B. A. (1998). Magnetic properties of modern soils and Quaternary loessic paleosols: paleoclimatic implications. *Palaeogeogr. Palaeoclimatol. Palaeoecol.* 137, 25–54. doi: 10.1016/S0031-0182(97)00103-X

Mastrolonardo, G., Francioso, O., and Certini, G. (2018). Relic charcoal hearth soils: a neglected carbon reservoir. Case study at Marsiliana forest, Central Italy. *Geoderma* 315, 88–95. doi: 10.1016/j.geoderma.2017.11.036

Mataix-Solera, J., Cerdà, A., Arcenegui, V., Jordán, A., and Zavala, L. M. (2011). Fire effects on soil aggregation: a review. *Earth Sci. Rev.* 109, 44–60. doi: 10.1016/j.earscirev.2011.08.002

Mikan, C. J., and Abrams, M. D. (1995). Altered forest composition and soil properties of historic charcoal hearths in southeastern Pennsylvania. *Can. J. Forest Res.* 25, 687–696. doi: 10.1139/x95-076

Müller, F. (2017). *Der Wandel der Kulturlandschaft im Raum Peitz infolge des mehrhundertjährigen Betriebes des dortigen Eisenhüttenwerkes (Mitte 16. bis 19. Jahrhundert)*, Cottbus.

Munsell (2009). *Munsell Soil- Color Charts*. Munsell Color, Grand Rapids.

Mylavarapu, R. S., Sanchez, J. F., Nguyen, J. H., and Bartos, J. M. (2002). Evaluation of Mehlich-1 and Mehlich-3 extraction procedures for plant nutrients in acid mineral soils of Florida*. *Commun. Soil Sci. Plan.* 33, 807–820. doi: 10.1081/CSS-120003067

Nornberg, P., Vendelboe, A. L., Gunnlaugsson, H. P., Merrison, J. P., Finster, K., and Jensen, S. K. (2009). Comparison of the mineralogical effects of an experimental forest fire on a goethite/ferrihydrite soil with a topsoil that contains hematite, maghemite and goethite. *Clay Miner* 44, 239–247. doi: 10.1180/claymin.2009.044.2.239

Pasmore, A. (1964). Surviving evidence of the New Forest charcoal burning industry. *J. Indus. Archaeol.* 1, 27.

Pèlachs, A., Nadal, J., Soriano, J., Molina, D., and Cunill, R. (2009). Changes in Pyrenean woodlands as a result of the intensity of human exploitation: 2,000 years of metallurgy in Vallferrera, northeast Iberian Peninsula. *Veg. Hist. Archaeobot.* 18, 403–416. doi: 10.1007/s00334-009-0218-6

Powell, A. J., Wheeler, J., and Batt, C. M. (2012). Identifying archaeological wood stack charcoal production sites using geophysical prospection: magnetic characteristics from a modern wood stack charcoal burn site. *J. Archaeol. Sci.* 39, 1197–1204. doi: 10.1016/j.jas.2011.11.005

Quednau, T., and Ludemann, T. (2017). First pedoanthracological study in the Black Forest, SW Germany. *Quat. Int.* 457, 131–139. doi: 10.1016/j.quaint.2017.03.014

Raab, A., Bonhage, A., Schneider, A., Raab, T., Rösler, H., Heußner, K.-U., et al. (in press). Spatial distribution of relict charcoal hearths in the former royal forest district Tauer (SE Brandenburg, Germany). *Quat. Int.* doi: 10.1016/j.quaint.2017.07.022

Raab, A., Takla, M., Raab, T., Nicolay, A., Schneider, A., Rösler, H., et al. (2015). Pre-industrial charcoal production in Lower Lusatia (Brandenburg, Germany): Detection and evaluation of a large charcoal-burning field by combining archaeological studies, GIS-based analyses of shaded-relief maps and dendrochronological age determination. *Quat. Int.* 367, 111–122. doi: 10.1016/j.quaint.2014.09.041

Raab, T., Hirsch, F., Ouimet, W., Johnson, K. M., Dethier, D., and Raab, A. (2017). Architecture of relict charcoal hearths (RCHs) in northwestern Connecticut, USA. *Geoarchaeology.* 32, 502–510. doi: 10.1002/gea.21614

Rösler, H., Bönisch, E., Schopper, F., Raab, T., and Raab, A. (2012). "Pre-industrial charcoal production in southern Brandenburg and its impact on the environment," in *Landscape Archaeology Between Art and Science: From a Multi- To an Interdisciplinary Approach,* eds S. Kluiving and E. Guttmann-Bond (Amsterdam: Amsterdam University Press - Landscape and Heritage Research), 167–178.

Rutkiewicz, P., Malik, I., Wistuba, M., and Sady, A. (2017). Charcoal kilns as a source of data on the past iron industry (an example from the River Czarna valley, Central Poland). *Environ. Socio Econ. Stud.* 5, 12. doi: 10.1515/environ-2017-0012

Schmidt, L. M., and Levy, J. S. (2017). Hydraulic conductivity of active layer soils in the McMurdo Dry Valleys, Antarctica: geological legacy controls modern hillslope connectivity. *Geomorphology* 283, 61–71. doi: 10.1016/j.geomorph.2017.01.038

Schmidt, M., Mölder, A., Schönfelder, E., Engel, F., and Fortmann-Valtink, W. (2016). Charcoal kiln sites, associated landscape attributes and historic forest conditions: DTM-based investigations in Hesse (Germany). *Forest Ecosyst.* 3:8. doi: 10.1186/s40663-016-0067-6

Schneider, A., Raab, A., Rösler, H., Takla, M., Hirsch, F., Ritschl, B., et al. (2016). Geophysikalische Prospektion und Mikrodrohnenbefliegungen zur Dokumentation von Meilerplätzen in der Jänschwalder Heide. *Arbeitsberichte zur Bodendenkmalpflege in Brandenburg* 30, 145.

Schneider, A., Takla, M., Nicolay, A., Raab, A., and Raab, T. (2015). A template-matching approach combining morphometric variables for automated mapping of charcoal kiln sites. *Archaeol. Prospect.* 22, 45–62. doi: 10.1002/arp.1497

Schwertmann, U. (1984). The double dehydroxylation peak of goethite. *Thermochim. Acta* 78, 39–46. doi: 10.1016/0040-6031(84)87130-0

Schwertmann, U. (1985). "The effect of pedogenic environments on iron oxide minerals," in *Advances in Soil Science,* ed B. A. Stewart (New York, NY: Springer), 171–200.

Stoops, G. (2003). *Guidelines for Analysis and Description of Soils and Regolith Thin Sections*. Madison, WI: Soil Science Society of America.

Straka, T. (2014). Historic charcoal production in the US and forest depletion: development of production parameters. *Adv. Hist. Stud.* 3, 104. doi: 10.4236/ahs.2014.32010

VDLUFA (2012). *Bestimmung von Phosphor und Kalium im Clacium-Acetat-Lactat-Auszug: Methodenhandbuch, I.* Darmstadt: VDLUFA-Verlag.

von Berg, C. H. E. (1860). *Anleitung zum Verkohlen des Holzes: ein Handbuch für Forstmänner, Hüttenbeamte, Technologen und Cameralisten.* Zernin.

von Kortzfleisch, A. (ed.). (2008). "Der klassische Platzmeiler," in *Die Kunst der Schwarzen Gesellen - Köhlerei im Harz* (Clausthal-Zellerfeld: Hermann-Reddersen-Stiftung), 42–54.

Wuenscher, R., Unterfrauner, H., Peticzka, R., and Zehetner, F. (2015). A comparison of 14 soil phosphorus extraction methods applied to 50 agricultural soils from Central Europe. *Plant Soil Environ.* 61, 86–96.